Available online at www.sciencedirect.com
ScienceDirect
Journal of the European Ceramic Society 26 (2006) 3799–3807
www.elsevier.com/locate/jeurceramsoc

Thermomechanical characteristics of calcium aluminate cement and sand tapes prepared by tape casting

Julien Soro, Agnès Smith *, Christian Gault

Ecole Nationale Supérieure de Céramique Industrielle (ENSCI), Groupe d'Etude des Matériaux Hétérogènes (GEMH) (EA 3178), 47 à 73 Avenue Albert Thomas, 87065 Limoges Cedex, France

Received 22 March 2005; received in revised form 9 November 2005; accepted 19 November 2005
Available online 14 February 2006

Abstract

The present paper concerns the mechanical characterization of calcium aluminate cement and sand tapes prepared by tape casting, including ultrasonic measurements of Young's modulus at high temperature and evaluation of four point flexural behavior after heat treatments in the range of 20–1400 °C. It is shown that dehydration strongly affects mechanical properties in the 400–900 °C range, but that treatments at temperatures higher than 1200 °C increase both Young's modulus and strength. By correlation with thermal and X-ray diffraction analyses, the evolutions of thermomechanical properties have been related to phase and microstructural changes when heating the material after hydration: conversion of hydrates and dehydration at low temperature, then, crystallization of C–A and C–A–S phases and finally sintering at the highest temperatures. In a last part, it is shown that the reinforcement by glass fibres enhances the mechanical properties, in particular in the temperature range of dehydration, and gives to the material a non-brittle behavior.

Keywords: Tape casting; Composites; Mechanical properties; CA cement; Cements

1. Introduction

Calcium aluminate cements (CAC's) are a variety of cementitious materials. They are made of aluminum and calcium oxides. These cements are known to resist aggressive environments such as acid or bacterial attacks, they can withstand high temperatures and they present resistance to abrasion and impact when mixed with appropriate aggregates. CAC's are also used in a large range of formulated mixes together with Portland cements, with a form of calcium sulphate or with both; these products usually find applications in the building industry.[1] The aim of the present work is an attempt to demonstrate the possibility of extending CAC's out of their traditional uses, in particular to process a low cost matrix for new thermostructural composites. In this respect, we have used a processing method classically used for ceramics, namely tape casting.

The paper starts with a short presentation of the tape-casting process and the environmental interest in applying it to the manufacture of cement-based tapes. In a wish to manufacture tapes with a reduced quantity of CAC's, slurries containing increasing quantities of sand have been cast and tested, in order to select the composition with the most satisfactory mechanical strength. Then, the behavior at high temperature of such a material has been evaluated, by performing ultrasonic measurements of Young's modulus on this specific composition, between room temperature and 1400 °C. Plausible chemical phenomena are proposed in order to interpret the variations of Young's modulus as a function of temperature. Finally, an example of application of this method to manufacture unidirectional composites reinforced by glass fibers is reported.

2. Experimental procedure

2.1. Tape-casting process and raw materials

Tape casting is a process which is used for the preparation of ceramic thick films with a thickness that ranges between 100 and 500 μm. It has been long applied in the domain of technical ceramics.[2] Some examples of applications are the manufacture of substrates made of alumina or aluminum nitride for electronic applications, or the preparation of composite materials

* Corresponding author. Tel.: +33 5 5545 2204; fax: +33 5 5579 0998.
E-mail address: a_smith@ensci.fr (A. Smith).

0955-2219/$ – see front matter © 2006 Published by Elsevier Ltd.
doi:10.1016/j.jeurceramsoc.2005.11.010

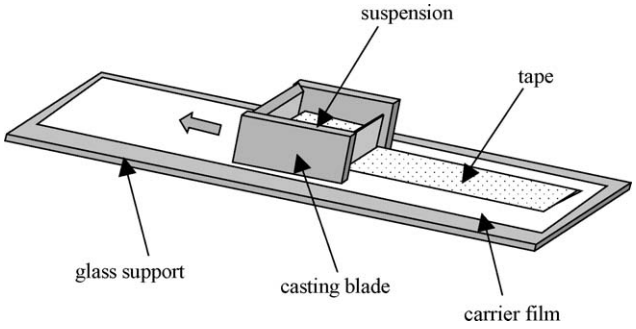

Fig. 1. Principle of the casting device used for processing cement–sand tapes.

for mechanical uses at high temperatures.[3] The slurry is a complex mixture, in a specific order, of powder, solvent, usually non-aqueous, dispersant, binder and plasticizer. Upon completion of mixing steps, a considerable quantity of either entrapped air or solvent vapor bubbles is usually present. De-airing is then necessary since bubbles in cast tapes act as initiation sites for cracks. The slurry is then cast on a surface to obtain a film. The following stage is de-binding to remove most organic components. It is usually done through a heat treatment at a moderate temperature (300–600 °C). The final step is sintering at high temperature in order to densify the tape. Compared to the case of technical ceramics, tape casting of cement-based compositions distinguishes itself by the following characteristics:[4]

(i) there is no need to use an organic solvent to prepare the slurry, it is replaced by water which also acts as a binder through the formation of hydrates;
(ii) hardening of cement-based tapes occurs at room temperature. No heat treatment at high temperature is required to sinter the material, in contrast to the situation for ceramic tapes made of technical ceramics. Therefore, compared to the manufacture of thick films of technical ceramics, tape-casting process applied to cementitious material is advantageous from the environmental point of view and is energy saving.

The process used for the fabrication of cement–sand tapes is described elsewhere.[5] The casting device is schematically presented in Fig. 1.

The calcium aluminate cement used in the present study is Secar 71 from Lafarge Aluminates. It mainly consists of calcium aluminate, $CaO{\cdot}Al_2O_3$ (noted CA)[1] and calcium dialuminate $CaO{\cdot}2Al_2O_3$ (noted CA_2).[1] Its particle size ranges between 0.1 and 100 μm with an average particle size of 12 μm. The sand comes from Fontainebleau (France). It is mostly silica (99.6 wt.%) and the particle size is between 10 and 100 μm with an average value of 70 μm.

The preparation of the slurry follows the steps reported in Fig. 2. The sequence of additions is critical. The dispersant has to be added before the binder and plasticizers to prevent competitive adsorption. The initial adsorption of the plasticizers and binder on the particle surfaces prevents the dispersant from being subsequently adsorbed, thereby decreasing its effectiveness.[5] The fractional volume of each constituent in the slurry mixture (sand, cement, dispersant, plasticizer, water) has been adjusted in order to obtain the best compromise between good casting properties (rheofluidizing behavior), and the optimization of the hydration process leading to satisfactory mechanical properties.

After casting, the tapes are immerged into water, using a specific procedure in order to achieve hydration of the cementitious mix. Two temperatures of water, 20 and 70 °C, leading to different hydration rates have been tested. After complete hydration (96 h at 20 °C and 12 h at 70 °C), the tapes of 10 cm in width and about 1.5 mm in thickness, can be machined into parallelepipedic samples for mechanical characterization.

2.2. Characterization methods

2.2.1. Ultrasonic measurements

Ultrasonic measurement as a function of temperature is a method which has been applied to investigate the behavior of refractory materials.[6] Among the different modes which can be used to propagate ultrasonic waves in solids, the "long bar" mode is well suited for performing velocity measurements at high temperature. The velocity of longitudinal waves in the long bar mode, V_{LBM}, is related to the macroscopic Young's modulus, E, of the propagation media through the relation:

$$V_{LBM} = \left(\frac{E}{\rho}\right)^{1/2} \quad (1)$$

where ρ is the density of the material.

The experimental setup used in the present study is presented on Fig. 3 and detailed elsewhere.[7] A transducer sends ultrasonic waves through an alumina waveguide. The dimensions of the parallelepipedic sample (length, $L = 120$ mm; lateral dimension, $D = 5$ mm and thickness, e = thickness of the tape) are optimized by taking into account the section of the waveguide and the thickness of the cast tape. The sample is glued on the waveguide with a high-temperature adhesive. The condition for propagation in the "long bar" mode is $D/\lambda \leq 0.2$, where λ is the wavelength. In our case, it corresponds to the propagation of ultrasonic waves at frequencies lower than 500 kHz.

The sample is introduced in a furnace (heating ramp: 5 °C min^{-1}; maximum temperature reached in the present study: 1400 °C; cooling ramp: 5 °C min^{-1}). The determination of ultrasonic velocity consists in measuring the round-trip time, τ, between two successive echoes in the sample, by an automatic signal processing system, USANALYS, made at the laboratory.[7]

At room temperature, the ultrasonic velocity, V_{LBM0}, is obtained from relation (2):

$$V_{LBM0} = \frac{2L_0}{\tau_0} \quad (2)$$

Therefore, Young's modulus at room temperature, E_0, is obtained by combining Eqs. (1) and (2).

[1] In the following, CaO, Al_2O_3, SiO_2 and H_2O are noted according to cementitous terminology C, A, S and H.

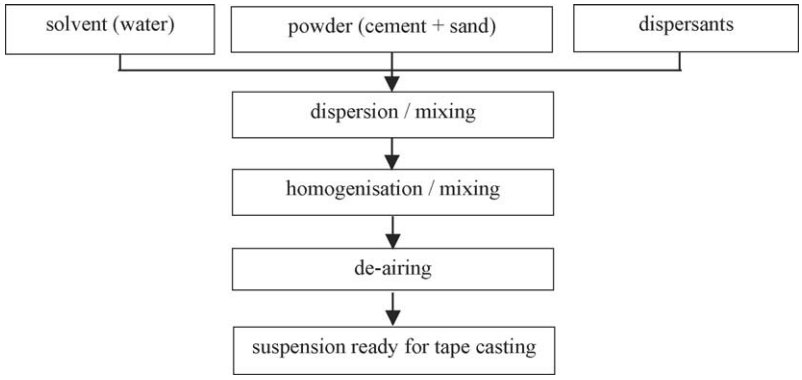

Fig. 2. Procedure for the preparation of tape casting suspensions.

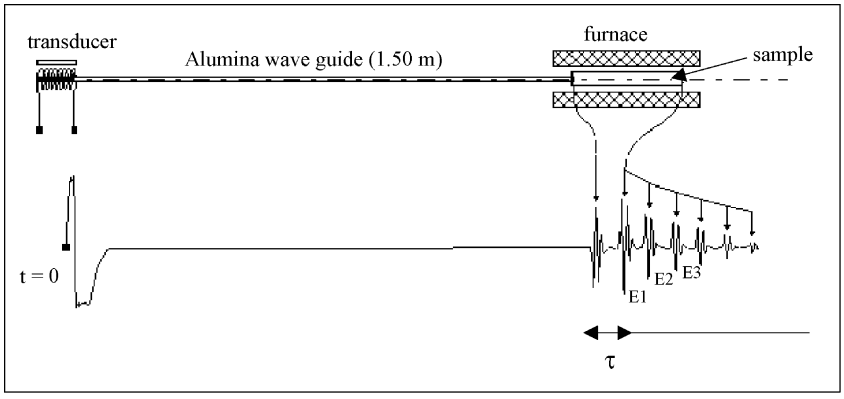

Fig. 3. Principle of the experimental setup for ultrasonic velocity measurements as a function of temperature.

At temperature T, the ultrasonic velocity $V_{LBM}(T)$ is given by:

$$V_{LBM}(T) = \frac{2L(T)}{\tau(T)} \tag{3}$$

where $L(T)$ and $\tau(T)$ are the values at temperature T of L and τ, respectively.

Eqs. (1) and (3) show that ultrasonic measurements can be used to follow the variations of E with temperature. When the length and the mass of the sample change during heating, because of thermal expansion and eventual chemical reactions, corrections have to be made from dilatometric and thermogravimetric experiments. Therefore, the relative variations of E at a given temperature can be written as:

$$\frac{E(T)}{E_0} = \left(\frac{\tau_0}{\tau}\right)^2 \left(1 - \frac{\Delta L(T)}{L_0}\right)\left(1 + \frac{\Delta m(T)}{m_0}\right) \tag{4}$$

where the suffix 0 is related to the values at room temperature, $\Delta m(T)/m_0$ and $\Delta L(T)/L_0$ are the variations, between room temperature and T, of mass and length, respectively.

The accuracy of measurement of τ is better than 0.5%.[7] Therefore, taking into account the experimental errors on measurements of density and length of the cement tapes samples, E was determined with an accuracy of about 2%. Nevertheless, relative variations of Young's modulus versus temperature can be followed by using Eq. (4) with a sensitivity better than 0.1%, provided the relative variations of length and mass are considered.

2.2.2. Flexural behavior measurements

For mechanical testing, we used an apparatus from J. J. Instruments S. A. (reference M30K), with a cell of 100 N, equipped with a four points bending test system (Fig. 4). The parallelepipedic specimen is resting on two simple supports separated by a distance u. A load is applied at two points, distant of v, symmetrical compared to the middle of the sample. Given the section $b \times h$ of the specimen (h is fixed by the thickness of the tape), the applied load, F_a, we can calculate the stress, σ, on the face in tension as follows:

$$\sigma = \frac{3F_a(u - v)}{bh^2} \tag{5}$$

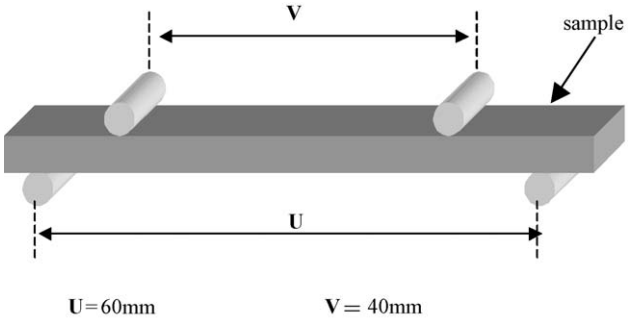

Fig. 4. Principle of measurement of four points bending tests.

By plotting σ versus the displacement, d, of the transverse bar of the testing machine, the mechanical behavior in flexion can be obtained.

The value of σ corresponding to the rupture of the sample gives the strength σ_R. For each sample, at least five measurements are carried out and data presented here correspond to average values of σ_R.

2.2.3. Thermal analyses

For thermal analyses, the heating ramp was 5 °C/min to 1400 °C and the cooling ramp was 5 °C/min. Variations of sample length with temperature were recorded by dilatometry (apparatus: Adamel Lhomargy, DI 24). Mass variations and differential thermal analysis (DTA) were recorded on 100 mg of product (apparatus: Setaram Setsys 24); the reference powder was an alumina from Prolabo (purity >98%).

2.2.4. X-rays diffraction (XRD)

XRD was carried out at room temperature with an INEL Curved Position Sensitive (CPS-120) diffractometer apparatus. Prior to XRD, each sample was heated at a given temperature between room temperature and 1400 °C (heating ramp: 5 °C/min, 30 min at the maximum temperature, cooling ramp: 5 °C/min).

3. Results and discussion

3.1. Characteristics of a tape made of cement and sand

Fig. 5 presents flexural strength measurements as a function of the sand content ratio, $M_{sand}/(M_{cement} + M_{sand})$, for tapes hydrated in water at 20 and 70 °C. Taking into consideration the error bars for each measurement, it shows that the strength increases up to about 25%, and decreases after 30%, both for hydration at 20 and 70 °C. Considering the cement–sand mix as a composite, this can be explained by the reinforcement of the cement matrix by sand particles which limits microcracking of the matrix during hydration. This effect is less efficient when the cement ratio drops to a critical value which is not sufficient to allow the formation of hydrates for a good bonding between

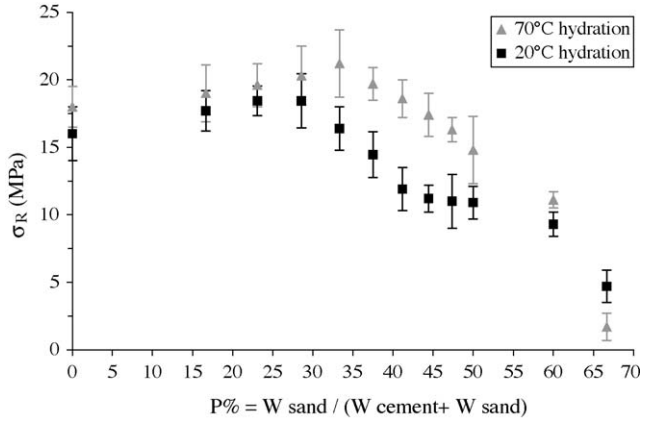

Fig. 5. Flexural strength measurements, σ_R, for tapes with increasing sand content, hydrated in water at two temperatures 20 and 70 °C.

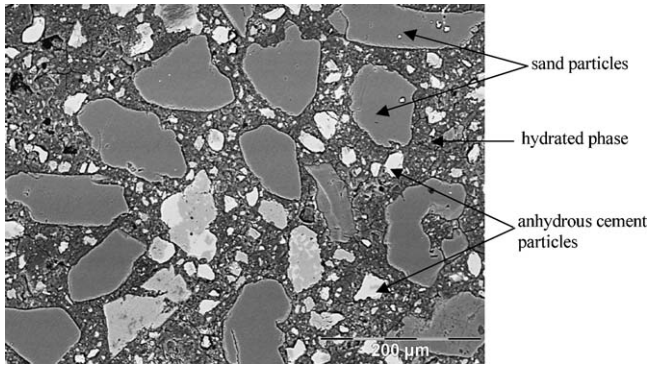

Fig. 6. SEM observation of a polished section of a hydrated tape with a 29% sand ratio.

particles. In the following, taking into account this, and also, that no significant increase of strength is observed between the two temperatures, results will be presented for compositions with a sand ratio equal to 29%, hydrated at 20 °C. Fig. 6 shows a SEM picture of a polished section of a tape of this composition. A regular distribution of the sand grains into the cement matrix with few microcracks is observed.

Fig. 7 shows ultrasonic measurements as a function of temperature for this selected composition. Distinctive zones can be identified when heating (zones 1–5) and then cooling (zone 6).

Zone 1 (room temperature to 175 °C): Young's modulus goes down from 24.5 to 19 GPa when the temperature rises to 125 °C. Between 125 and 175 °C, E increases to 21 GPa.

Phenomena occurring in this temperature range are well documented in the literature. Nonnet et al.[8] studied the elastic properties of refractory castables containing some aluminous cement as the binding phase. They proposed the following events: the decrease of modulus is associated with the conversion of CAH_{10} (reactions 1 and 2, Table 1). DTA measurements on these samples confirm that between room temperature and 175 °C, CAH_{10} decomposes through an endothermal reaction (Fig. 8a). The loss of mechanical characteristics is only transient since the modulus increases again when $T > 125$ °C because of the hydration

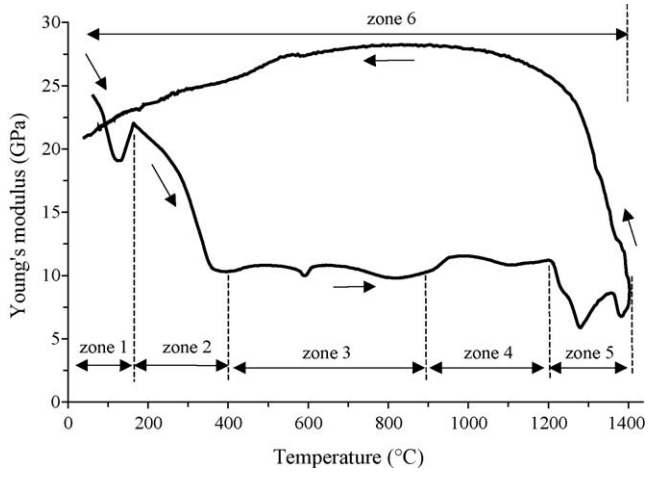

Fig. 7. Variations of Young's modulus as a function of temperature for a tape with a sand ratio of 29%, hydrated into water at 20 °C.

Table 1
Summary of different possible chemical reactions

Reactions	Number
$3CAH_{10} \rightarrow C_3AH_6 + 2AH_3 + 18H$	1
$2CAH_{10} \rightarrow C_2AH_8 + AH_3 + 9H$	2
$3CA + 12H \rightarrow C_3AH_6 + 2AH_3$	3
$3C_2AH_8 \rightarrow 2C_3AH_6 + AH_3 + 9H$	4
$AH_3 \rightarrow A + 3H$	5
$7C_3AH_6 \rightarrow C_{12}A_7(H) + 9CH + 32H$	6
$CA + A \rightarrow CA_2$	7

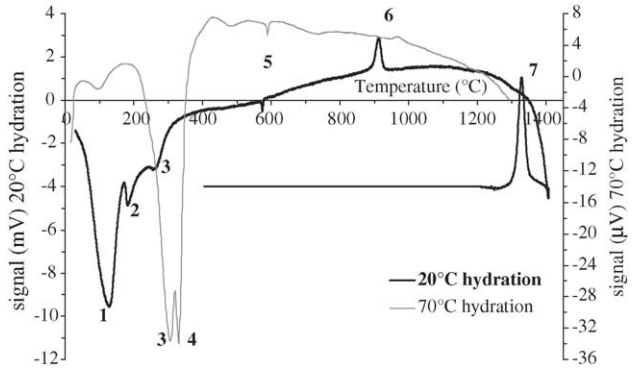

Fig. 8. DTA measurements of tapes with 29% of sand content hydrated into water at 20 °C and 70 °C. Peaks identification: (1) dehydration of CAH_{10}; (2) dehydration of C_2AH_8; (3) dehydration of AH_3; (4) dehydration of C_3H_6; (5) transformation of α-quartz into β-quartz; (6) crystallization of CA; (7) crystallization of CAS_2 and C_2AS.

of remaining anhydrous CA (reaction 3, Table 1) with water produced from reactions 1 and 2.

Zone 2 (175–400 °C): the modulus decreases to 11 GPa.

This decrease corresponds to successive events. Between 175 and about 275 °C, we assume that C_2AH_8 decomposes through reaction 4 (Table 1) to give C_3AH_6 and AH_3. C_2AH_8 can originate from two sources: (i) it is already in the set samples. XRD spectra indicate the presence of crystalline C_2AH_8 in these specimens (Table 2); (ii) it comes from the conversion of CAH_{10} in zone 1 (reaction 2, Table 1).

Around 275 °C and above, DTA results show an endothermal peak. This could possibly be explained by the decomposition of AH_3 and C_3AH_6 formed during reactions 1–4. In order to check this point, DTA measurements were carried out on samples left to set at 70 °C, i.e. at a temperature where C_3AH_6 forms (Fig. 8a). Two distinctive endothermal peaks exist between 200 and 400 °C, which are associated to the decomposition of AH_3 and C_3AH_6 according to reactions 5 and 6 (Table 1), respectively.[9]

These dehydration mechanisms are accompanied by microcracking and porosity formation which explain the decrease of elastic properties.

Zone 3 (400–900 °C): Young's modulus presents little variation, except around 573 °C due to the endothermal transformation of α-quartz into β-quartz as shown on the DTA curve (Fig. 8).

In this range, few structural changes occur: CH coming from reaction 6 dehydrates at 450 °C.[9] Moreover, XRD data (Table 2) show that crystalline $C_{12}A_7$ is present in samples heated between 400 and 900 °C. During this step, relatively low and constant values of *E* are measured, of the order of 10 GPa and the tapes exhibit, as usual for materials with hydraulic binders, after dehydration, very weak mechanical properties.

Zone 4 (900–1200 °C): *E* starts increasing when *T* goes from 900 to 950 °C and remains around 11–12 GPa afterwards.

As it is known in literature,[6] crystallization phenomena generally involve increases of elastic properties, because atomic bonds are stiffer in crystals than in amorphous structures. The increase of *E* in zone 4, is associated with the crystallization of CA as evidenced by the exothermal peak that starts at 900 °C. Though no quantitative dosage of the different crystalline phases has been done, Table 2 shows that the relative peak intensity associated to CA is greater in samples heated at 1000 °C than at lower temperatures. If we assume, in a first approximation, that, for a given crystalline phase, the relative intensity of the diffraction peaks is proportional to its quantity, the more CA is present in the material, the greater is the modulus.

From 1100 °C, there is a slight increase in *E*. It can be due to the reaction between CA and *A* originating from reaction 7 (Table 1) to give CA_2, which is stiffer than CA.[8] Actually, at 1200 °C, we can notice a decrease (respectively increase) of the most intensive diffraction peak relative to CA (respectively, CA_2).

Zone 5 (1200–1400 °C): *E* first decreases between 11.5 and 6 GPa when the temperature increases between 1200 and

Table 2
Percentages of intensities of the most intensive diffraction peaks of the different crystalline phases present in a tape with 29% of sand content, after thermal treatments

	20 °C	300 °C	400 °C	500 °C	600 °C	700 °C	800 °C	900 °C	1000 °C	1200 °C	1300 °C	1350 °C	1400 °C
CAH_{10}	3.76	0	0	0	0	0	0	0	0	0	0	0	0
C_2AH_8	1.18	0	0	0	0	0	0	0	0	0	0	0	0
C_3AH_6	0.90	7.79	3.32	0	0	0	0	0	0	0	0	0	0
AH_3	1.38	1.66	0.84	0	0	0	0	0	0	0	0	0	0
$C_{12}A_7$	0	0	0	2.67	1.47	1.92	2.75	3.22	0	0	0	0	0
CA	10.75	7.77	7.89	11.74	8.84	7.29	7.52	7.88	19.59	18.73	19.02	3.95	9.58
CA_2	9.89	7.89	5.90	10.71	8.68	7.96	7.53	6.94	13.04	17.79	24.17	11.49	21.95
A	2.49	1.87	2.28	3.06	4.42	3.17	1.76	1.70	2.16	1.45	1.59	3.51	22.34
SiO_2	69.64	74.90	79.77	71.83	76.58	79.66	80.44	80.25	65.21	56.68	43.86	56.61	7.2
C_2AS	0	0	0	0	0	0	0	0	0	3.12	6.74	11.11	8.49
CAS_2	0	0	0	0	0	0	0	0	0	2.23	4.62	13.33	29.74

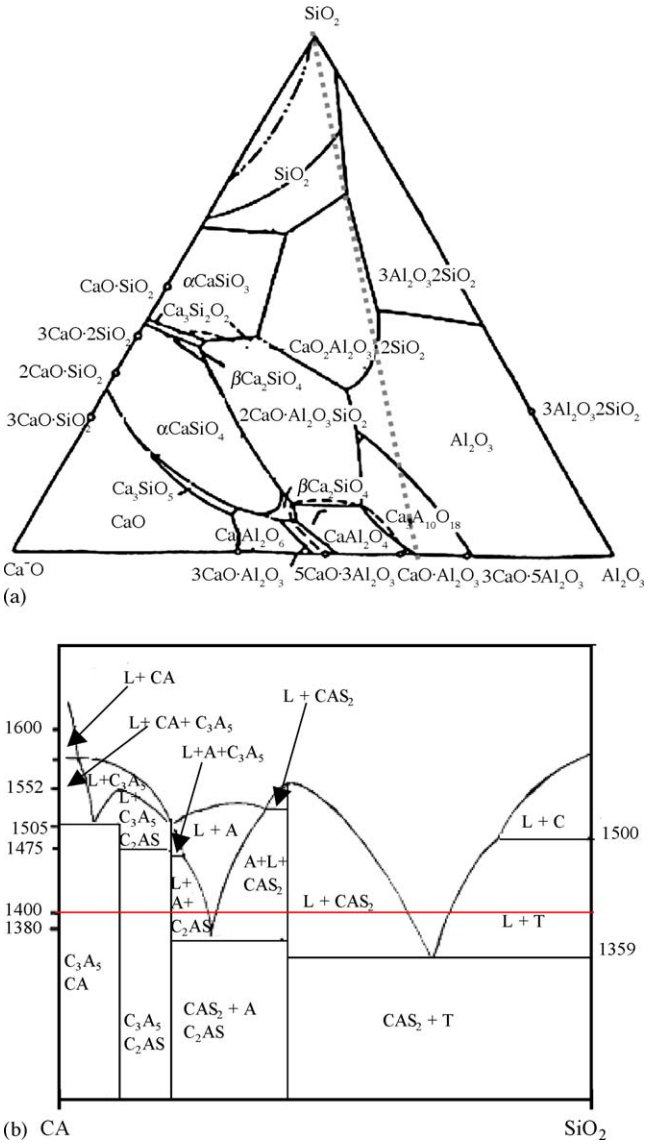

Fig. 9. (a) Ternary phase diagram between SiO_2, CaO and Al_2O_3. (b) Pseudo-binary phase diagram deduced from (a).

1280 °C. Thereafter, E goes up to 9 GPa at $T = 1365$ °C and drops to 6 GPa when T approaches 1400 °C.

For interpretation, one has to refer to the ternary phase diagram between CaO, Al_2O_3 and SiO_2 (Fig. 9a). There are two eutectic points at 1170 and 1265 °C, respectively. The drop of E between 1200 and 1280 °C is attributed to the formation of liquid phases which increases the visco-elastic character. The pseudo-binary diagram between CA and S (Fig. 9b) shows that solid phases, namely anorthite, CAS_2, gehlenite, C_2AS, and alumina can form: XRD on samples heated at 1350 °C provides evidence for the presence of these crystalline phases. Therefore, the formation of these crystalline phases causes the increase in E. Beyond 1359 °C, Fig. 9b indicates the formation of a liquid phase and the consequence is a drop in E.

Zone 6 (1400 °C down to room temperature): during sample cooling, E goes up and reaches maximum values of 29 GPa around 900 °C.

DTA curve upon cooling shows an exothermal peak that starts at 1359 °C (Fig. 8). On cooling, the liquid phase transforms into different crystalline phases with high elastic properties: XRD spectra on a sample heated at 1400 °C and cooled down to room temperature give evidence for the presence of these different phases (CAS_2, C_2AS). Moreover, crack healing by liquid phases at high temperature increases the stiffness of the material when cooling. Lastly, the drop of E on cooling between 900 °C and room temperature can be explained by microcracking because of thermal expansion mismatch. The micrograph and EDS analyses of a polished section of a tape treated at 1400 °C (Fig. 10) show the microstructure with sintered crystallized phases (responsible of the increase of elastic properties at high temperature) and the presence of cracks (which involve the decrease of E when cooling).

Fig. 11 gives the results of measurements of flexural strength at 20 °C for samples previously heated at different temperatures. As expected, it decreases when the materials have been dehydrated and remains minimal between 400 and 1200 °C. In agreement with results of elastic measurements, it increases once the sample is heated above the temperature where the material becomes stiffer and reaches values around 30–32 MPa.

3.2. Application to the fabrication of composites reinforced with glass fibres

In order to demonstrate the potentiality of tape casting to elaborate composites with cementitious matrices, this section reports results obtained in tapes reinforced with long glass fibers (Vetrotex, from Saint-Gobain). These fibers were chosen because of their low cost and their good resistance to the alkaline elements of the cements: they were found to be well suited to make composites working at low temperature (inferior to the glass transition temperature of 650 °C). Before their use, fibres were chemically desized.

The process procedure is detailed elsewhere.[5] In particular, the rheology of the suspension has to be adjusted, in order to present a Newtonian behaviour to easily impregnate the fibre strands, while remaining sufficiently plastic to preserve a homogeneous and regular thickness after casting. Unidirectional mono-layers (called prepregs) were fabricated by casting a first matrix layer. Then, a layer of fibres was superimposed, tightened between two combs, before casting of a second layer of matrix with the same thickness as the first one. After 1 h of hydraulic setting in the open air on the support, the prepreg was hydrated by immersion in water at 20 °C during 96 h, which helps hydration and material consolidation. The tape is then cut into square $10 \times 10\,cm^2$ sheets which can be piled up and cemented to each other by a thin film of the same slurry as the one used for tape casting, in order to obtain, after hydration, 1D or 2D 0°/90°/0° stratified composites.

Fig. 12 gives a schematic representation of a prepreg. By changing the inter-tows distance, it is possible to obtain fibre fractional volume ranging from 1.4 to 15%. It was found that 11% leads to the best compromise between a good infiltration of the matrix into tows and a good mechanical reinforcement. A SEM picture of a polished section of a hydrated

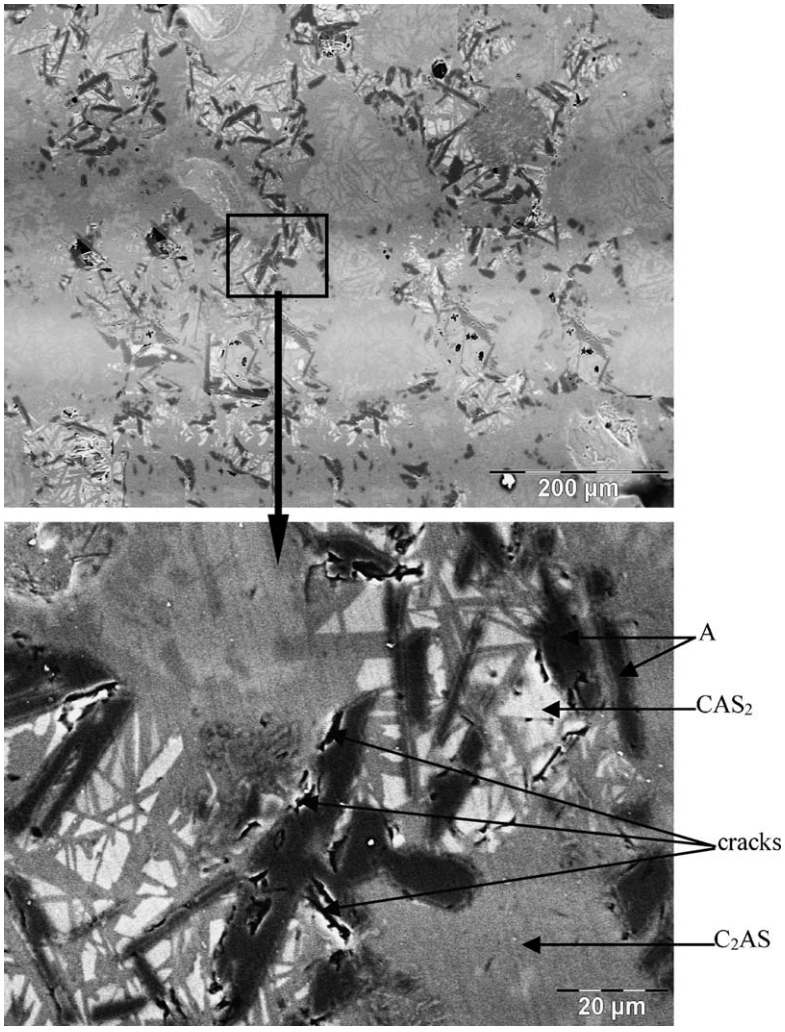

Fig. 10. SEM observation of polished section of a tape after heat treatment at 1400 °C.

prepreg with 11% fractional volume of glass fibre is given in Fig. 13.

Fig. 14 shows the result of four points bending tests performed on a sample of cement–sand composition alone and on a prepreg with the same matrix composition, respectively, after hydration. The effect of the reinforcement of material by fibres is quite obvious: not only the four points bending resistance of prepreg increases by approximately a factor 3 compared to that of the matrix, but also the mechanical behavior curve exhibits a large non-linear section, which is typical of a ceramic-ceramic non-brittle composite.[10]

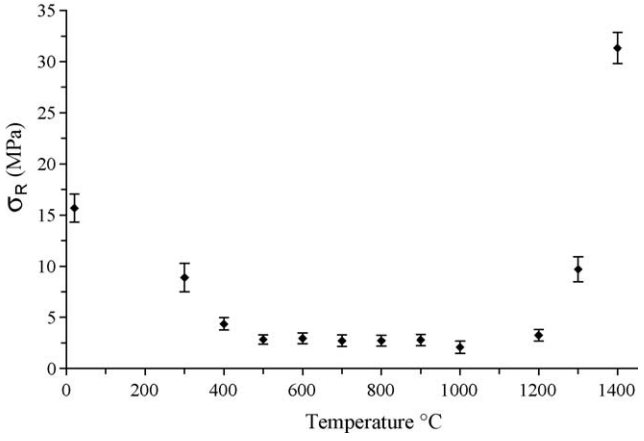

Fig. 11. Flexural strength measured at room temperature as a function of temperature of thermal treatment, for tapes with 29% of sand content, hydrated into water at 20 °C.

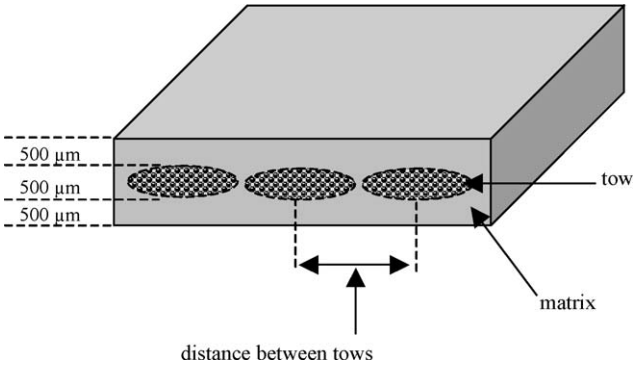

Fig. 12. Schematic representation of a prepreg section.

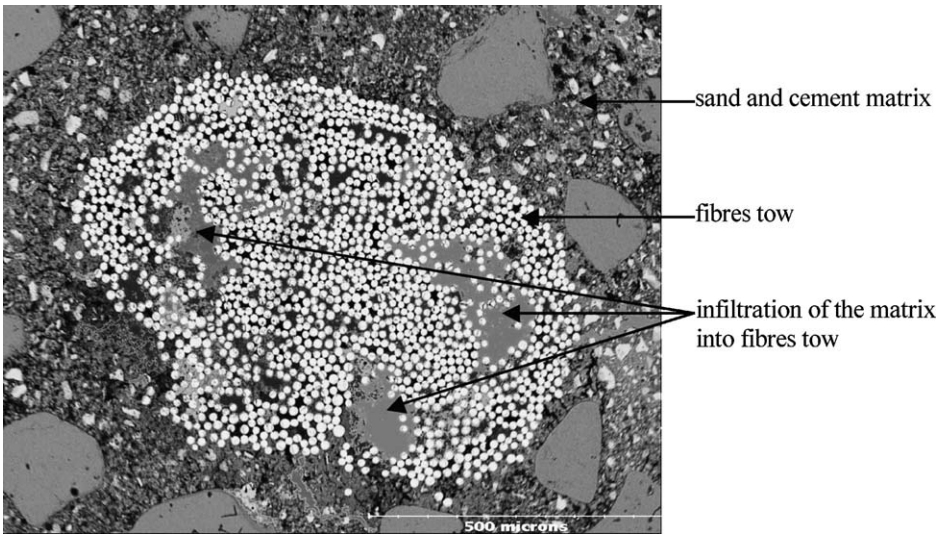

Fig. 13. SEM picture of a polished section of an hydrated prepreg showing the infiltration of the cement–sand matrix into a glass fibre tow.

The study of the behavior of composites versus temperature has been limited up to 600 °C, which corresponds to the maximum temperature of use of the fiber. Variations of Young's modulus in a 1D composite, made of two prepregs, are presented

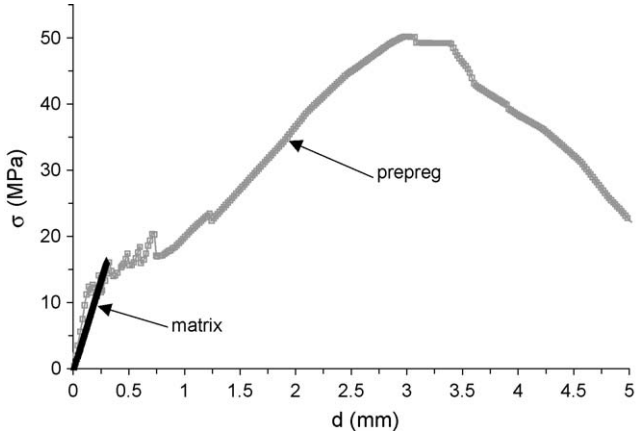

Fig. 14. Flexural behavior at 20 °C of a cement–sand tape and of a prepreg with the same matrix composition.

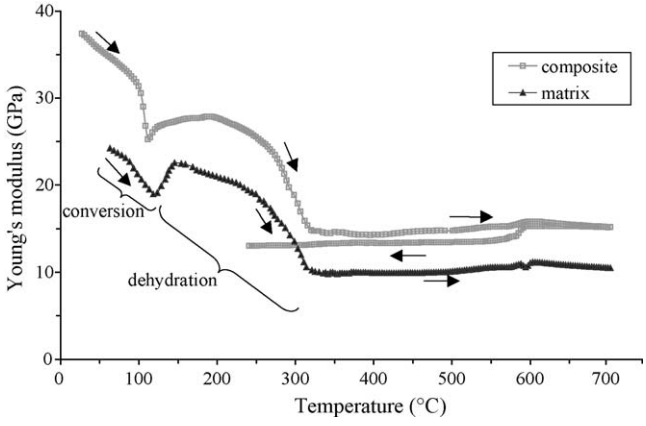

Fig. 15. Young's modulus evolutions vs. *T* in a cement–sand tape and in a prepreg with the same matrix composition.

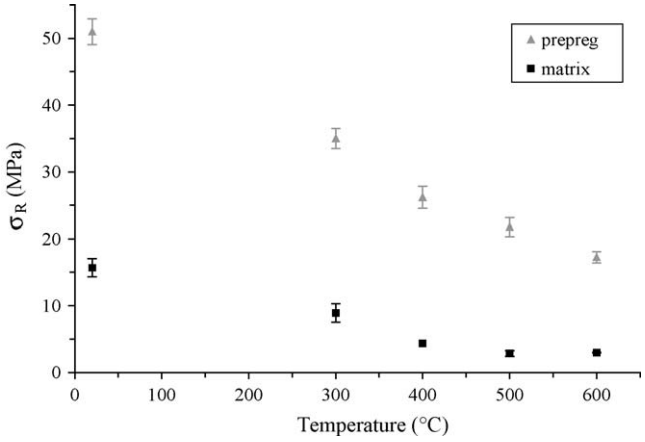

Fig. 16. Flexural strength measured at 20 °C vs. the temperature treatment for a cement–sand tape and for a prepreg with the same matrix composition.

in Fig. 15 and compared to the result obtained in the same conditions for the cement–sand matrix (Fig. 7). The effects of structural transformations in the cementitious matrix, as described above in zone 1, zone 2 and the beginning of zone 3, are also observed in the prepreg, but the modulus remains higher (about 50%) for the composite because of the presence of fibres.

The decrease of mechanical properties after dehydration is confirmed by the decrease of the measured strength at 20 °C after heat treatments up to 600 °C (Fig. 16). Nevertheless, it is important to note the strong effect of the fibre reinforcement: though, after heating at 400 °C, the strength of the matrix drops to a very low value (<5 MPa), the strength for a prepreg is maintained at more than 25 MPa after the same treatment.

4. Conclusion

Microstructural evolutions of alumina cement–silica sand layers processed by tape casting have been investigated by ultrasonic high temperature measurements between room temperature and 1400 °C. The different mechanisms responsible of the

main mechanical property variations have been identified: dehydration, crystallization of CA, CA_2, CAS_2 and C_2AS, formation of liquid phases, sintering. It is demonstrated that such layers can be used as matrix to process low cost composite plates by tape casting. An example of reinforcement of a layer by glass fibres is reported, which shows that the mechanical behavior becomes non-brittle and that the flexural strength is strongly increased by the fibres. These results are now to be used to process composite plates with high temperature fibres for thermostructural applications.

References

1. Scrivener, K. and Van Damme, H., Construction materials: from innovation to conservation. *Mater. Res. Soc. Bull.*, 2004, **29**(5), 308–310.
2. Chartier, T., *Tape casting, in Encyclopedia of advanced materials*. Pergamon Press, 1994, 2763–2768.
3. Lostec, L., Chartier, T., Gault, C. and Larnac, G., SiC fibre-reinforced ceramic matrix composites: processing by tape casting and properties. *Key Eng. Mater.* (*Vol 127–131*). Trans. Tech. Publ., Switzerland, 1997, pp. 303–312.
4. El Hafiane, Y., *Coulage en bande de ciment alumineux*. Ph.D. thesis, University of Limoges, France, 2002.
5. Soro, J., *Elaboration par coulage en bande et caractérisation de composites fibreux à matrice à base de ciment*. Ph.D. thesis, University of Limoges, France, 2005.
6. Gault, C., Ultrasonic non destructive evaluation of microstructural changes and degradation of ceramics at high temperature. *Mater. Res. Soc. Symp. Proc.* (*Vol 142*), ed. J. Holbrook and J. Bussière, 1989, pp. 263–274.
7. Huger, M., Fargeot, D. and Gault, C., High-temperature measurement of ultrasonic wave velocity in refractory materials. *High Temp.-High Pressure*, 2002, **34**, 193–201.
8. Nonnet, E., Lequeux, N. and Boch, P., Elastic properties of high alumina cement castables from room temperature to 1600 °C. *J. Eur. Ceram. Soc.*, 1999, **19**, 1575–1583.
9. Richard, N., *Structure et propriétés des phases cimentières à base de mono-aluminate de calcium*. Ph.D. thesis, University of Paris, VI, France, 1996.
10. Prewo, K. M., Fibre-reinforced ceramics: new opportunities for composite materials. *Ceram. Bull.*, 1989, **68**(2), 395–400.